

# Optimization of Power Solar Dish-Stirling: Induced Effects of Heat Source Temperature and Working Fluid Temperature in Hot Side

Mohammad H. Ahmadi<sup>1,\*</sup>, Hosyen Sayyaadi<sup>2</sup>

<sup>1</sup>Renewable Energies and Environmental Department, Faculty of New Science and Technologies, University of Tehran, Tehran, Iran

<sup>2</sup>Faculty of Mechanical Engineering-Energy Division, K.N. Toosi University of Technology, Tehran, Iran

\*Corresponding author: mohammadhosein.ahmadi@gmail.com

Received March 31, 2014; Revised May 04, 2014; Accepted May 04, 2014

**Abstract** This paper presents an investigation on finite time thermodynamic evaluation and analysis of a Solar-dish Stirling heat engine. Finite time thermodynamics has been applied to determine the net power output and thermal efficiency of the Stirling system with finite-rate heat transfer, regenerative heat loss, conductive thermal bridging loss and finite regeneration process time. The model investigates the effects of the inlet temperature of the heat source and heat sink, the volumetric ratio of the engine, effectiveness of heat exchangers and heat capacitance rates on the net power output and thermal efficiency of the engine and entropy generation. The thermal efficiency of the cycle corresponding to the magnitude of the maximized power of the engine is evaluated. Finally, sensitivities of results in a variation of the thermal parameters of the engine are studied. The present analysis provides a good theoretical guideline for designing and operating of the Stirling heat engine systems.

**Keywords:** *stirling engine, thermal efficiency, entropy generation, solar dish, concentration ratio*

**Cite This Article:** Mohammad H. Ahmadi, and Hosyen Sayyaadi, "Optimization of Power Solar Dish-Stirling: Induced Effects of Heat Source Temperature and Working Fluid Temperature in Hot Side." *Sustainable Energy*, vol. 2, no. 3 (2014): 91-101. doi: 10.12691/rse-2-3-3.

## 1. Introduction

The Stirling engine is a simple type of external-combustion engine that uses a compressible fluid as a working fluid. The Stirling engine can theoretically be a very efficient engine to convert heat into mechanical work at Carnot efficiency. The thermal limit for the operation of a Stirling engine depends on the material used for its construction. In most instances, the engines operate with a heater and cooler temperature of 923 and 338 K, respectively [1]. Engine efficiency ranges from about 30 to 40% resulting from a typical temperature range of 923–1073 K, and normal operating speed range from 2000 to 4000 rpm [2].

The classical analysis of the operation of real Stirling engines is that of Schmidt [3]. The theory provides for harmonic motion of the reciprocating elements, but retains the major assumptions of isothermal compression and expansion and perfect regeneration. It thus remains highly idealized, but is certainly more realistic than the ideal Stirling cycle [4].

Senft [5] developed an engine with 2°C temperature difference due to analysis on rotary mechanism. Senft [6] studied Crossley-Stirling engine that is described by two isochoric and two polytropic processes and presented an optimum compression ratio. Also he studied thermodynamic performance and physical restrictions

while mechanical efficiency as function of volumetric ratio, temperature ratio and effectiveness of regenerator was developed [7]. Organ was studied effects of various parameters such as diameter, length and materials on regenerator performance, irreversibilities and temperature gradient in Stirling engine regenerator while regenerator was optimized [8,9]. Formosa and Despesse [10] modeled engine's output power and efficiency due to dead volume by implementing of the isotherm model.

Thombare and, Verma [11] gathered the available technologies and obtained achievements with regard to the analysis of Stirling engines and, at the end, presented some suggestions for their applications.

Tavakolpour et al. [12], experimentally investigated gamma type solar engine by implementing a flat plate solar collector which has 80C temperature difference and 900 W.m<sup>-2</sup> density solar radiation can generate 1.2 W of output power in 30 rpm rotation speed. Ahmadi et al [13] Investigated of Solar Collector Design Parameters Effect onto Solar Stirling Engine Efficiency.

Shendage et. al [14] analyzed a rhombic feature for the design of a single cylinder, beta type Stirling engine of 1.5 kWe capacity for rural electrification. Eid [15] showed the performance of a beta-configuration heat engine having a regenerative displacer. The theoretical analysis of the engine is based mainly on Schmidt theory, the objective for the optimum looking dimensions. In comparison between the proposed engine which has a regenerative more power with more efficiency than the GPU-3 engine.

Podesser [16] investigated heated alpha type Stirling engine by applying flue gas in the outlet of biomass furnace. In their engine, the engine pressure was 33 bar and 600 rpm rotation speed which leads to produce 3.2 kW output power. Costae and Feidt [17] explored the effect of the variation of the overall heat transfer coefficient on the optimum state and on the optimum distribution of the heat transfer surface conductance in the area of the heat exchangers of the Stirling engine. Makhkamov [18] has formed mathematical and practical examination of working process and mechanical losses of a 1kW Stirling engine manufactured for solar operation. Also, He has also emphasized the necessity of simulation of the engine process for better understanding into the engine system.

A thermodynamic analysis of a gamma-type Stirling engine by using a quasi-steady flow model was implemented by Parlak, et al. [19].

Cinar et al. [20] constructed a beta-type Stirling engine which operate at atmospheric pressure. The tests performed on this engine have indicated that by increasing the heat source temperature, the engine speed, engine torque, and power output will be increased.

Minassians et al., constructed and studied the performance of Stirling engine with low temperature solar collector to generate power and heat [21]. A more complete theoretical model of a LTD Stirling engine developed by Robson et al. [22]. In this model, a full differential description of the major components of the engine, the behavior of the gas in the expansion and the compression spaces, the behavior of the gas in the regenerator, the dynamic behavior of the displacer, and the power piston/flywheel assembly was investigated.

Kongtragool [23] studied the influence of the regenerator efficiency and the dead volumes on the work as well as the efficiency of the machine. However, this study does not include the heat transfers through the temperature difference at the heat source and sink.

In 2005, Kongtragool and Wongwises [24] analyzed, theoretically, the power output of the gamma-configuration LTD Stirling engine. The former works on Stirling-engine power output calculation were considered and discussed. They indicated that the mean pressure power formula was the most appropriate for LTD Stirling-engine power output estimation. However, the hot-space and cold-space working fluid temperature was needed in the mean-pressure power formula. In 2005, Kongtragool and Wongwises [25] organized the optimum absorber temperature of a once-reflecting full-conical reflector for a LTD Stirling engine. A mathematical model for the overall efficiency of a solar-powered Stirling engine was developed. Both limiting conditions of maximum possible engine efficiency and power output were considered. Results disclosed that the optimum absorber temperatures obtained from both conditions were not significantly different and the overall efficiency in the case of the maximum possible engine power output was very close to that of the real engine of 55% Carnot efficiency.

The idea of coupling of solar concentrators to Stirling engines is a new technology which facilitates conversion of the solar energy into the electric power. In this regard a dish collector with the parabolic arrangement of its mirrors is used to concentrate the sun radiations in a focal point of the collector which the heat absorber of the

engine is located i.e. the solar energy is collected and concentrated thanks to a parabola of mirrors.

For solar applications, Abdullah et al. [26] have presented the design considerations to be taken into account in designing a low-temperature differential double-acting Stirling engine.

On the basis of the conventional entropy techniques, for the studying of solar Stirling engine cycle performance, Costea et al. [27] included the effects of heat transfers, incomplete heat regeneration and irreversibilities of the cycle as conduction, pressure losses or mechanical friction between the moving parts. Timoumi et al. [28] developed an exact second order model counting all the losses at the same time. The method based on a lumped analysis approach leads to a numerical model and has been applied for the optimization of the General Motors GPU-3 [29,30].

The development of finite-time thermodynamics [31,32,33,34], a new discipline in modern thermodynamics, provides a powerful tool for performance analysis of practical engineering cycles. Several authors have studied the finite-time thermodynamic performance of the Stirling engine [35-42]. Ahmadi et al [35,36,37] developed an intelligent approach to figure power of solar Stirling heat engine by implementation of evolutionary algorithms Blank and Wu [38] studied the power output and thermal efficiency of a finite time, optimized, extra-terrestrial, solar-radiant Stirling heat engine, in which the heat source and sink were assumed to have infinite heat-capacity rates, obtaining expressions for optimum power and efficiency at optimum power.

Li et al developed a mathematical model for the overall thermal efficiency of solar powered high temperature differential dish Stirling engine with finite heat transfer and the irreversibility of regenerator and optimized the absorber temperature and corresponding thermal efficiency [39]. Tlili investigated effects of regenerating effectiveness and heat capacitance rate of external fluids in a heat source / sink at maximum power and efficiency [40]. Kaushik et al studied the effects of irreversibilities of regeneration and heat transfer of heat/sink sources [41,42].

In the present work by utilizing the finite time thermodynamic analysis method, the thermal efficiency of the system and the entropy generation correspond to output system power in order to discover the optimized design of the Stirling are analyzed.

The analysis investigates the sensitivity of the system operational variables against the maximum output power, Stirling thermal efficiency, entropy generation and thermal efficiency of the dish system.

## 2. System Description

In a solar - dish Stirling systems, mirrors of the parabolic shaped concentrator focuses the sunlight to the focal point of the concentrator where the hot end of the Stirling engine is located. Therefore, the solar energy with a relatively high temperature is transferred to the hot side heat exchanger of the Stirling engine. Figure 1 illustrates a schematic for a solar-dish Stirling engine connected to a solar dish concentrator. The solar-dish is equipped with a sun tracker which tracks the sun in order to have maximum solar energy transfer to the engine when the sun moves during the days. Hence, solar energy is absorbed

and transferred to the working fluid in the hot space of an engine.

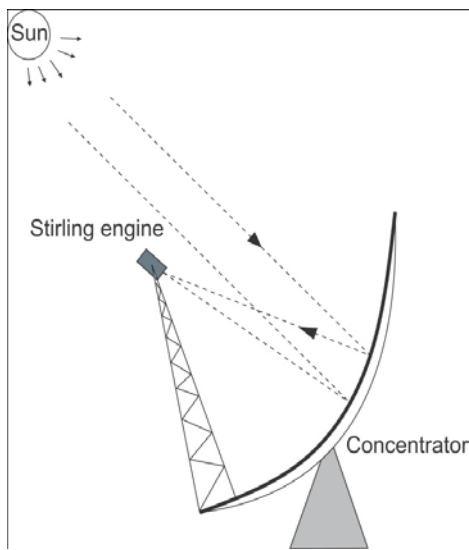


Figure 1. Schematic of a solar Stirling engine

Figure 2 is a schematic diagram of a Stirling heat engine cycle with finite-time heat transfer and regenerative heat losses. As shown in Figure 3, Stirling cycle consisted of four processes. Process 1-2 is an isothermal process, in which the working fluid after compressing at constant temperature,  $T_c$  and rejected heat to the heat sink at low temperature  $T_{L1}$ , Therefore, the temperature of heat sink is increased to  $T_{L2}$ . Then the working fluid crosses over the regenerator and warms up to  $T_h$  in an isochoric process 2-3. In process 3-4, the working fluid is expanded in a constant temperature  $T_h$  process and receives heat from the heat source in which its temperature is reduced from  $T_{H1}$  into  $T_{H2}$ . Last process (4-1), is an isochoric cooling process, where the regenerator absorbs heat from the working fluid.

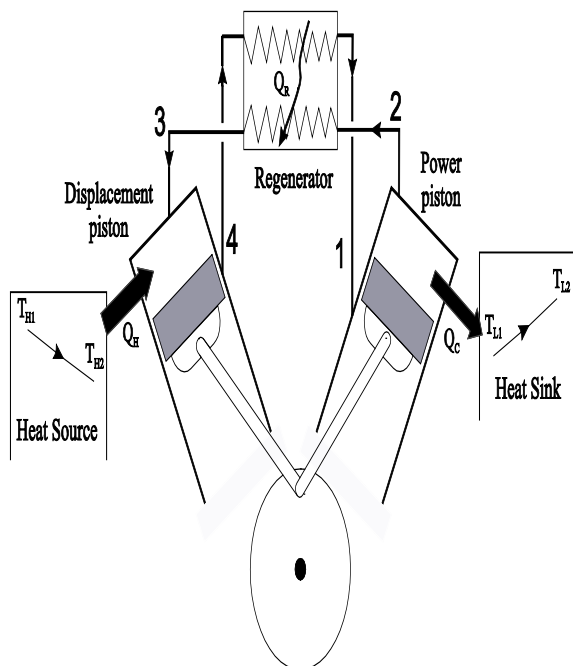


Figure 2. Schematic diagram of the Stirling heat engine cycle

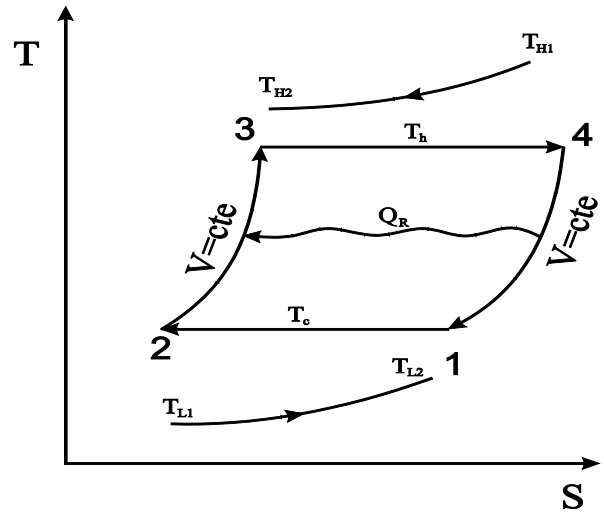


Figure 3. T-S diagram of a Stirling engine cycle

In a real cycle it is impractical to have an ideal heat transfer in the regenerator in which entire amount of absorbed heat (in the process 4-1) is transferred to the working fluid in the heating mode (process 2-3). Therefore a heat transfer loss denoted by  $\Delta Q_R$  is occurred in the regenerator. In addition, a conduction heat transfer between the heat source and the heat sink namely as thermal bridge loss ( $Q_0$ ) must be considered.

### 3. Thermodynamic Analysis of the System

The actual useful heat gain of the dish collector, considering conduction, convection and radiation losses is given by [25,39] as follows:

$$q_u = IA_{app}\eta_0 - A_{rec}[h(T_{H_{ave}} - T_0) + \varepsilon\delta(T_{H_{ave}}^4 - T_0^4)] \quad (1)$$

where  $I$  is the direct solar flux intensity,  $A_{app}$  is the collector aperture area,  $\eta_0$  is the collector optical efficiency,  $A_{rec}$  is the absorber area,  $h$  is conduction/convection heat transfer coefficient,  $T_{H_{ave}}$  is the average absorber temperature,  $T_0$  is the ambient temperature,  $\varepsilon$  is an emissivity factor of the collector,  $\delta$  is the Stefan's constant.

The thermal efficiency  $\eta_s$  of the dish collector is obtained as [25,39]:

$$\eta_s = \frac{q_u}{IA_{app}} = \eta_0 - \frac{1}{IC}[h(T_{H_{ave}} - T_0) + \varepsilon\delta(T_{H_{ave}}^4 - T_0^4)] \quad (2)$$

#### 3.1. Regenerative Heat Losses in the Regenerator

It is important to mention that there also exists a finite heat transfer in the regenerative heat transfer ( $Q_R$ ) is given by [39,40,41,42]:

$$Q_r = nC_v\varepsilon_R(T_h - T_c) \quad (3)$$

$\Delta Q_r$  is the heat loss during the two regenerative processes in the cycle. By the following relationship is obtained [39,40,41]:

$$\Delta Q_r = nC_v(1 - \varepsilon_R)(T_h - T_c) \quad (4)$$

$n$  is the mass of the working fluid in mole,  $C_v$  is the specific heat capacity of the working fluid in the regenerative processes in terms of mole,  $\varepsilon_r$  is the effectiveness of regenerator,  $T_h$  and  $T_c$  are the working fluid temperatures in the hot space and cold space, respectively.

Owing to the influence of irreversibility of the finite-rate heat transfer, the time of the regenerative processes is not negligible in comparison to that of the two isothermal processes [37,38,39]. In order to calculate the time of the regenerative processes, one assumes that the temperature of the working fluid in the regenerative processes as a function of time is given by [37,38,39]:

$$\frac{dT}{dt} = \pm M_i \quad (5)$$

where  $M$  is the proportionality constant which is independent of the temperature difference and dependent only on the property of the regenerative material, called regenerative time constant and the  $\pm$  sign belong to the heating ( $i=1$ ) and cooling ( $i=2$ ) processes respectively [37,38,39].

$$t_3 = \frac{T_1 - T_2}{M_1} \quad (6)$$

$$t_4 = \frac{T_1 - T_2}{M_2} \quad (7)$$

### 3.2. The Amounts of Heat Released by the Heat Source and Absorbed by the Heat Sink

The heat released between heat source and working fluid ( $Q_h$ ), the heat absorbed between the working fluid and the heat sink ( $Q_c$ ) is obtained as follows:

$$Q_h = nRT_h Ln\lambda + nC_v(1 - \varepsilon_R)(T_h - T_c) \quad (8)$$

$$Q_c = nRT_c Ln\lambda + nC_v(1 - \varepsilon_R)(T_h - T_c) \quad (9)$$

On the other hand

$$Q_h = \left[ C_H \varepsilon_H (T_{H1} - T_h) + \xi C_H \varepsilon_H (T_{H1}^4 - T_h^4) \right] t_h \quad (10)$$

$$Q_c = C_L \varepsilon_L (T_c - T_{L1}) t_l \quad (11)$$

where  $C_H$  and  $C_L$  are the heat capacitance rate of external fluids in the heat source and heat sink, respectively.

$$\varepsilon_H = 1 - e^{-N_H} \quad (12)$$

$$\varepsilon_L = 1 - e^{-N_L} \quad (13)$$

where  $\varepsilon_H$  and  $\varepsilon_L$  are the effectiveness's of the high and low temperature heat exchangers, respectively.

where  $N_L = \frac{U_L A_L}{C_L}$ ,  $N_H = \frac{U_H A_H}{C_H}$

#### The cyclic period

Using Eqs. (3)-(11), we get that the cyclic period  $t$  is:

$$t = \frac{nRT_h Ln\lambda + nC_v(1 - \varepsilon_R)(T_h - T_c)}{C_H \varepsilon_H (T_{H1} - T_h) + \xi C_H \varepsilon_H (T_{H1}^4 - T_h^4)} + \frac{nRT_c Ln\lambda + nC_v(1 - \varepsilon_R)(T_h - T_c)}{C_L \varepsilon_L (T_c - T_{L1})} + \left( \frac{1}{M_1} + \frac{1}{M_2} \right) (T_h - T_c) \quad (14)$$

### 3.3. The Conductive Thermal Bridging Losses from Heat Source to the Heat Sink

This value is proportional to the average temperature difference of the heat source and heat sink and the cycle time it is obtained as follows:

$$Q_o = K_o (T_{H_{ave}} - T_{L_{ave}}) t_{cycle} \quad (15)$$

$$T_{H_{ave}} = \frac{T_{H1} + T_{H2}}{2} \quad (15a)$$

$$T_{L_{ave}} = \frac{T_{L1} + T_{L2}}{2} \quad (15b)$$

We have [41,42]

$$T_{H2} = (1 - \varepsilon_H) T_{H1} + \varepsilon_H T_h \quad (15c)$$

$$T_{L2} = (1 - \varepsilon_L) T_{L1} + \varepsilon_L T_c \quad (15b)$$

Thus, using Eqs.(15a)-(15d), we have

$$Q_o = \frac{K_o}{2} \left[ (2 - \varepsilon_H) T_{H1} - (2 - \varepsilon_L) T_{L1} \right] t_{cycle} + (\varepsilon_H T_h - \varepsilon_L T_c) t_{cycle} \quad (16)$$

The net heat released from the heat source ( $Q_H$ ) and the net heat absorbed by the heat sink ( $Q_L$ ) are obtained as follows:

$$Q_H = Q_h + Q_o \quad (17)$$

$$Q_L = Q_c + Q_o \quad (18)$$

Considering the cyclic period of the Stirling engine, the output power, the thermal efficiency and entropy production of the engine are given by:

$$p = \frac{W}{t} = \frac{Q_H - Q_L}{t} \quad (19)$$

$$\eta_t = \frac{Q_H - Q_L}{Q_H} \quad (20)$$

$$\sigma = \frac{1}{t} \left( \frac{Q_L}{T_{L_{ave}}} - \frac{Q_H}{T_{H_{ave}}} \right) \quad (21)$$

Substituting Eqs. (3)- (14) into Eqs. (19) and (20) we have,

$$P = \frac{nR(T_h - T_c) Ln\lambda}{nRT_h Ln\lambda + nC_v(1 - \varepsilon_R)(T_h - T_c)} + \frac{C_H \varepsilon_H (T_{H1} - T_h) + \xi C_H \varepsilon_H (T_{H1}^4 - T_h^4)}{nRT_c Ln\lambda + nC_v(1 - \varepsilon_R)(T_h - T_c)} + \frac{nRT_c Ln\lambda + nC_v(1 - \varepsilon_R)(T_h - T_c)}{C_L \varepsilon_L (T_c - T_{L1})} + \left( \frac{1}{M_1} + \frac{1}{M_2} \right) (T_h - T_c) \quad (22)$$

$$\eta_t = \frac{nR(T_h - T_c)Ln\lambda}{nRT_hLn\lambda + nC_v(1 - \varepsilon_R)(T_h - T_c)} \quad (23)$$

$$+ \frac{K_o}{2} \left[ \frac{(2 - \varepsilon_H)T_{H_1} - (2 - \varepsilon_L)T_{L_1}}{+(\varepsilon_H T_h - \varepsilon_L T_c)} \right] t_{\text{cycle}}$$

With simplification and considering  $M = \frac{C_v(1 - \varepsilon_R)}{RLn\lambda}$

and  $F = \frac{1}{nR \ln \lambda} \left( \frac{1}{M_1} + \frac{1}{M_2} \right)$  we obtain:

$$P = \frac{T_h - T_c}{T_h + M(T_h - T_c)} \quad (24)$$

$$\frac{C_H \varepsilon_H (T_{H_1} - T_h) + \xi C_H \varepsilon_H (T_{H_1}^4 - T_h^4)}{C_H \varepsilon_H (T_{H_1} - T_h) + \xi C_H \varepsilon_H (T_{H_1}^4 - T_h^4)}$$

$$+ \frac{T_c + M(T_h - T_c)}{C_L \varepsilon_L (T_c - T_{L_1})} + F(T_h - T_c)$$

$$\eta_t = \frac{T_h - T_c}{T_h + M(T_h - T_c) + \frac{K_o}{2} \left[ \frac{(2 - \varepsilon_H)T_{H_1} - (2 - \varepsilon_L)T_{L_1}}{+(\varepsilon_H T_h - \varepsilon_L T_c)} \right]} \quad (25)$$

$$\left[ \frac{T_h + M(T_h - T_c)}{C_H \varepsilon_H (T_{H_1} - T_h) + \xi C_H \varepsilon_H (T_{H_1}^4 - T_h^4)} + \frac{T_c + M(T_h - T_c)}{C_L \varepsilon_L (T_c - T_{L_1})} + F(T_h - T_c) \right]$$

For the sake of convenience, a new parameter  $x = \frac{T_c}{T_h}$  is

introduced into Eqs. (24) and (25), then we have:

$$P = \frac{(1-x)}{\left( \frac{1+M(1-x)}{C_H \varepsilon_H (T_{H_1} - T_h) + \xi C_H \varepsilon_H (T_{H_1}^4 - T_h^4)} + \left( \frac{x+M(1-x)}{C_L \varepsilon_L (xT_h - T_{L_1})} \right) + F(1-x) \right)} \quad (26)$$

$$\eta_t = \frac{(1-x)}{1+M(1-x) + \frac{K_o}{2} \left[ \frac{(2 - \varepsilon_H)T_{H_1} - (2 - \varepsilon_L)T_{L_1}}{+(\varepsilon_H - x\varepsilon_L)} \right]} \quad (27)$$

$$\left[ \frac{1+M(1-x)}{C_H \varepsilon_H (T_{H_1} - T_h) + \xi C_H \varepsilon_H (T_{H_1}^4 - T_h^4)} + \left( \frac{x+M(1-x)}{C_L \varepsilon_L (xT_h - T_{L_1})} \right) + F(1-x) \right]$$

For the optimization for maximum Power, Eq. (26) must be differentiated from  $T_h$  and put it equal to zero:

$$\frac{\partial P}{\partial T_h} = 0 \quad (28)$$

$$K_1 T_{h_{opt}}^8 + K_2 T_{h_{opt}}^5 + K_3 T_{h_{opt}}^4 + K_4 T_{h_{opt}}^3 + K_5 T_{h_{opt}}^2 + K_6 T_{h_{opt}} + K_7 = 0 \quad (29)$$

where

$$K_1 = \zeta^2 C_H^2 \varepsilon_H^2 B_1 x \quad (29a)$$

$$K_2 = \zeta C_H \varepsilon_H x (2C_H \varepsilon_H B_1 - 3B_2 C_L \varepsilon_L x) \quad (29b)$$

$$K_3 = 2\zeta C_H \varepsilon_H x (3B_2 C_L \varepsilon_L T_L - B_1 B_3) \quad (29c)$$

$$K_4 = -3B_2 \zeta C_H \varepsilon_H C_L \varepsilon_L T_L^2 \quad (29d)$$

$$K_5 = C_H \varepsilon_H x (B_1 C_H \varepsilon_H - B_2 x C_L \varepsilon_L) \quad (29e)$$

$$K_6 = 2C_H \varepsilon_H x (B_2 C_L \varepsilon_L T_L - B_1 B_3) \quad (29f)$$

$$K_7 = B_1 x B_3^2 - B_2 C_H \varepsilon_H C_L \varepsilon_L T_L^2 \quad (29g)$$

$$B_1 = x + M(1-x) \quad (29h)$$

$$B_2 = 1 + M(1-x) \quad (29i)$$

$$B_3 = C_H \varepsilon_H T_H + \zeta C_H \varepsilon_H T_H^4 \quad (29j)$$

With Placement  $T_{h_{opt}}$  in  $P_{\max}$  and  $\eta$ , maximum power and its corresponding thermal efficiency are calculated as follows:

$$P = \frac{(1-x)}{\left( \frac{1+M(1-x)}{C_H \varepsilon_H (T_{H_1} - T_{h_{opt}}) + \xi C_H \varepsilon_H (T_{H_1}^4 - T_{h_{opt}}^4)} + \left( \frac{x+M(1-x)}{C_L \varepsilon_L (xT_{h_{opt}} - T_{L_1})} \right) + F(1-x) \right)} \quad (30)$$

$$\eta_t = \frac{(1-x)}{1+M(1-x) + \frac{K_o}{2} \left[ \frac{(2 - \varepsilon_H)T_{H_1} - (2 - \varepsilon_L)T_{L_1}}{+(\varepsilon_H - x\varepsilon_L)} \right]} \quad (31)$$

$$\left[ \frac{1+M(1-x)}{C_H \varepsilon_H (T_{H_1} - T_{h_{opt}}) + \xi C_H \varepsilon_H (T_{H_1}^4 - T_{h_{opt}}^4)} + \left( \frac{x+M(1-x)}{C_L \varepsilon_L (xT_{h_{opt}} - T_{L_1})} \right) + F(1-x) \right]$$

The maximum thermal efficiency of the entire solar-dish Stirling engine is a product of the thermal efficiency of the collector and the optimal thermal efficiency of the Stirling engine [39]. Namely:

$$\eta_m = \eta_s \eta_t \quad (32)$$

Therefore by substituting of Eqs. (2) And (31) into Eq. (32), we have the following expression for thermal efficiency of the entire solar-dish Stirling engine:

$$\eta_m = \left\{ \eta_0 - \frac{1}{IC} [h(T_{H1} - T_0) + \varepsilon \delta (T_{H1}^4 - T_0^4)] \right\} \frac{(1-x)}{1 + M(1-x) + \frac{K_o}{2} \left[ \frac{(2-\varepsilon_H)T_{H1} - (2-\varepsilon_L)T_{L1}}{+T_{hopl}(\varepsilon_H - x\varepsilon_L)} \right]} \left[ \frac{1 + M(1-x)}{C_H \varepsilon_H (T_{H1} - T_{hopl}) + \zeta C_H \varepsilon_H (T_{H1}^4 - T_{hopl}^4)} \right] + \left[ \frac{x + M(1-x)}{C_L \varepsilon_L (xT_{hopl} - T_{L1})} \right] + F(1-x) \right\} \quad (33)$$

#### 4. Numerical Results and Discussion

In order to evaluate the effect of the heat source working fluid inlet temperature ( $T_{H1}$ ), heat capacitance rates ( $C_L, C_H$ ), the effectiveness of the regenerator ( $\varepsilon_R$ ), effectiveness of the heat exchangers ( $\varepsilon_H, \varepsilon_L$ ) and the heat

leak coefficient ( $k_0$ ) on the powered Stirling heat engine system, all the other parameters will be kept constant as  $x = 0.5$ ,  $C_H = C_L = 150 \text{WK}^{-1}$ ,  $n = 1 \text{mol}$ ,  $\lambda = 2$ ,  $R = 4.3 \text{Jmol}^{-1} \text{K}^{-1}$ ,  $C_v = 15 \text{Jmol}^{-1} \text{K}^{-1}$ ,  $\varepsilon_L = 0.7$ ,  $\varepsilon_H = 0.7$ ,  $\varepsilon_R = 0.9$ ,  $T_{L1} = 288 \text{K}$ ,  $T_{H1} = 1300 \text{K}$ ,  $T_0 = 288 \text{K}$ ,  $C = 1300$ ,  $\delta = 5.67 \times 10^{-8} \text{W.m}^{-2} \cdot \text{K}^{-4}$ ,  $h = 20 \text{W.m}^{-2} \cdot \text{K}^{-1}$ ,  $I = 1000 \text{W.m}^{-2}$ ,  $\varepsilon = 0.9$ ,  $\eta_0 = 0.9$ .

In the Figure 4 different system parameters against the heat source working fluid inlet temperature in the different heat capacities rate of the heat source are plotted. And in these figures by increasing the heat source working fluid temperature, maximum output power, Stirling thermal efficiency and entropy generation will be raised. Also the overall thermal efficiency of the dish system reaches a peak at about 900K and after that decreases. In Addition, at the given heat source working fluid inlet temperature all parameters (the maximum output power, Stirling thermal efficiency, entropy generation and thermal efficiency of the dish system) have increased with increasing of the heat capacities rate of the heat source.

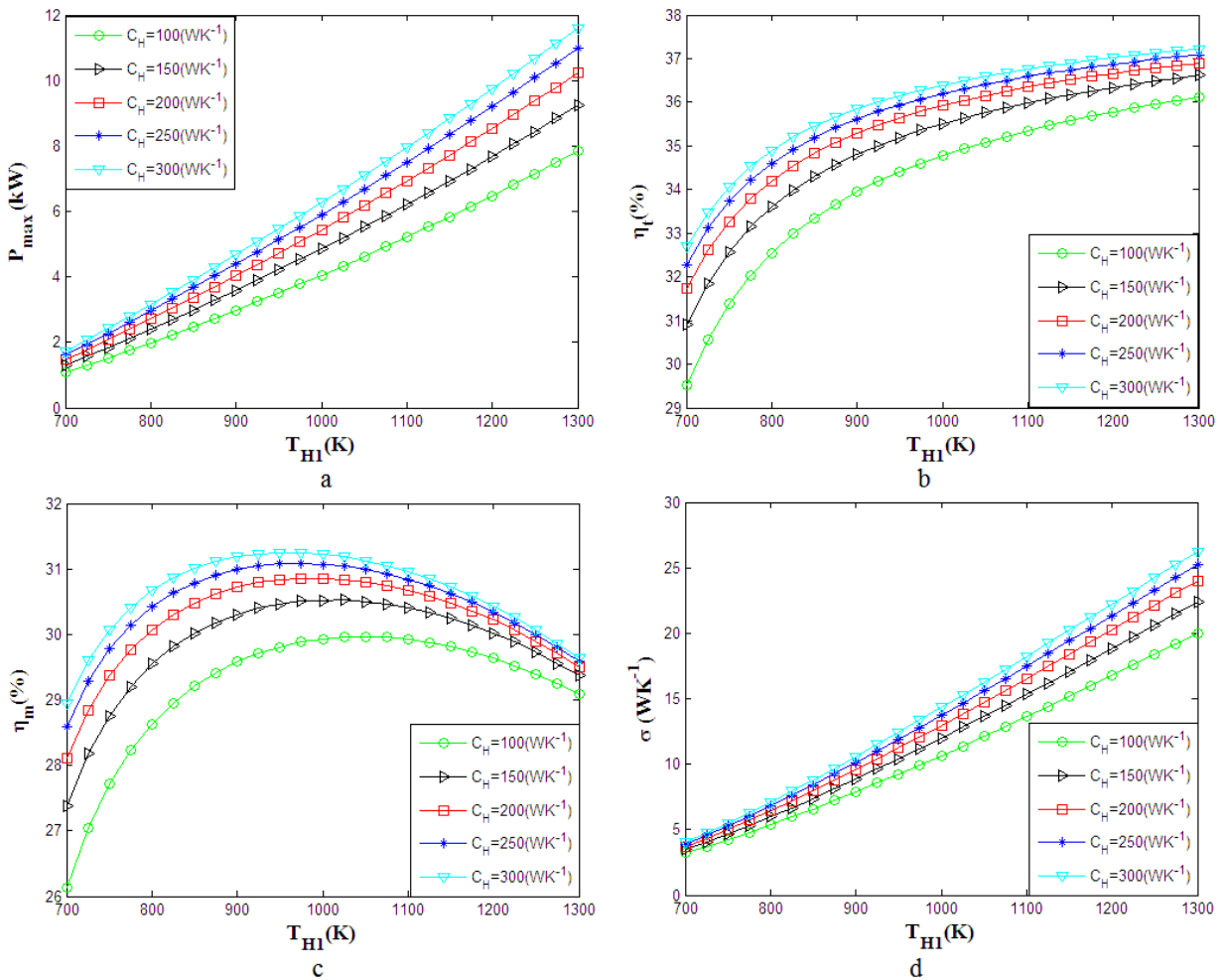


**Figure 4.** Variation of (a) maximum output power, (b) Stirling thermal efficiency, (c) thermal efficiency of the dish system and (d) entropy generation with heat source working fluid inlet temperature at a different heat capacities rate of heat source

In the Figure 5, all discussed parameter in Figure 4 are illustrated for the heat capacities rate of the heat sink. Surprisingly all parameters show the same trend against the heat source working fluid inlet temperature.

Furthermore at given heat source working fluid inlet temperature, all mentioned parameters increase with increasing the of the heat capacities rate of the heat sink.

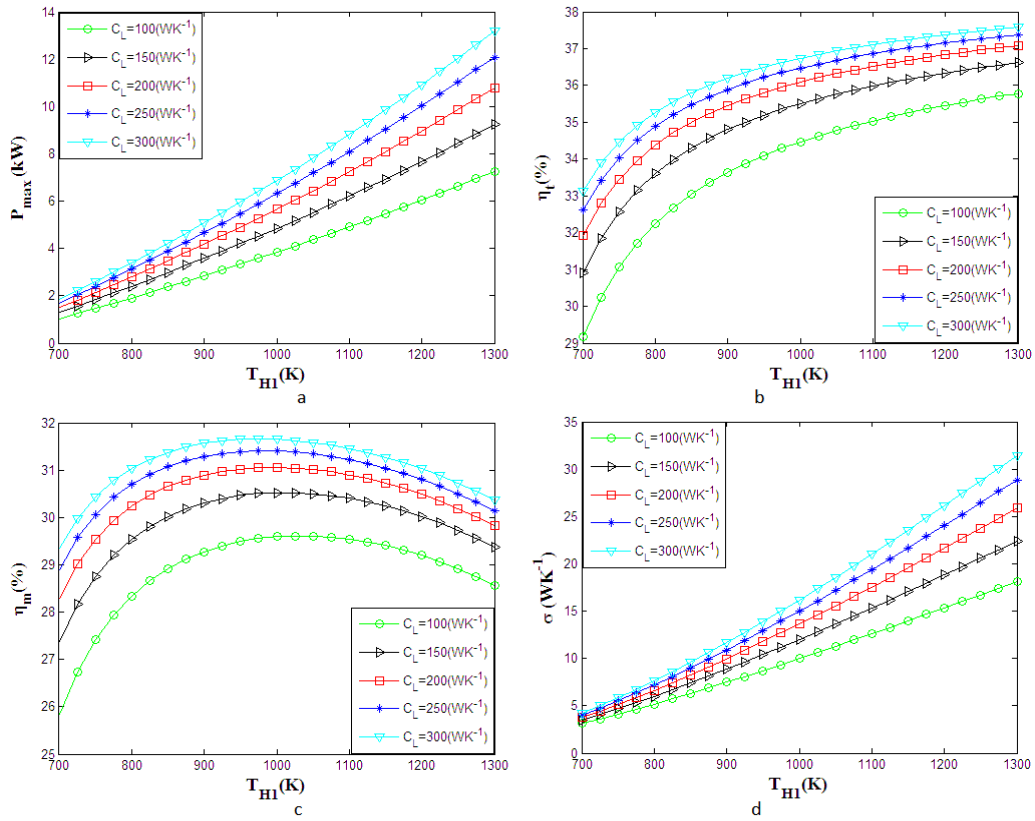


**Figure 5.** Variation of maximum (a) output power, (b) Stirling thermal efficiency, (c) thermal efficiency of the dish system and (d) entropy generation with heat source working fluid inlet temperature in the different heat capacities rate of heat sink

From Figure 6 it can be seen that, the maximum output power, the thermal efficiency and entropy generation increase considerably with increasing of the heat source working fluid inlet temperature at various values of the

hot side heat exchanger effectiveness (0.4-0.6). But the thermal efficiency of the Stirling dish system in the temperature of about 1000K reaches a maximum and then decreases.

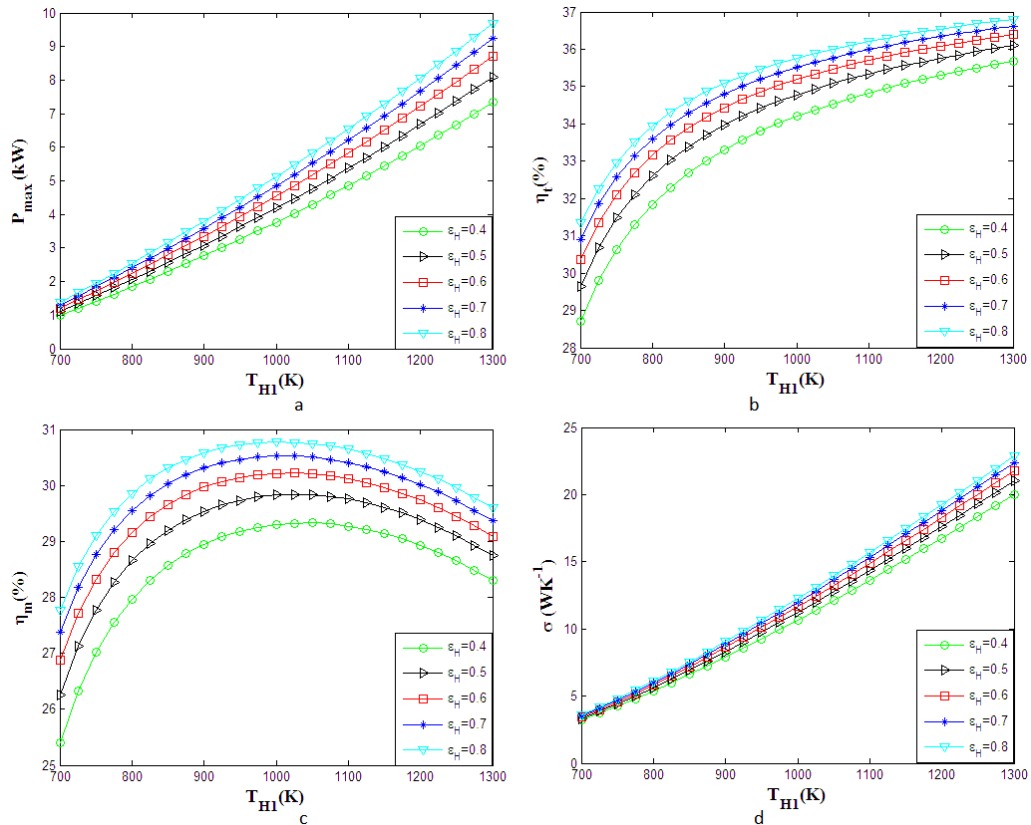


**Figure 6.** Effects of heat source working fluid inlet temperature and effectiveness of the hot side heat exchanger on the maximum (a) output power, (b) Stirling thermal efficiency, (c) thermal efficiency of the dish system and (d) entropy generation

Also in the Figure 7 the similar demonstrated parameters in the Figure 6 are plotted against the heat source working fluid inlet temperature at the different

effectiveness of the cold side heat exchanger. As it can be seen overall trends are the same as Figure 6.

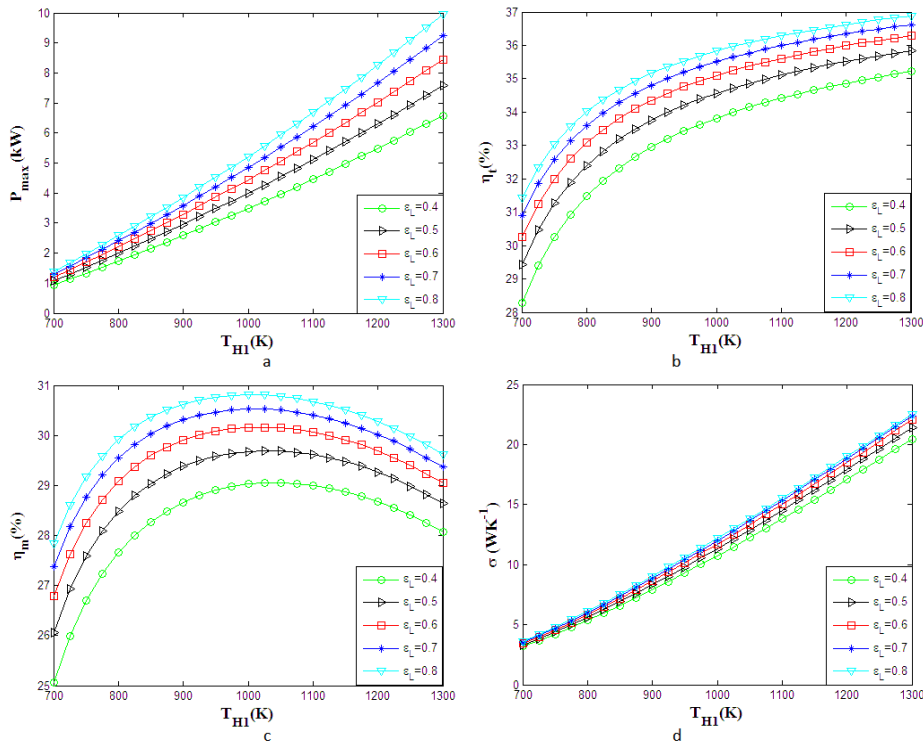


**Figure 7.** Effects of heat source working fluid inlet temperature and effectiveness of the cold side heat exchanger on the (a) maximum output power, (b) Stirling thermal efficiency, (c) thermal efficiency of the dish system and (d) entropy generation

In the Figure 8 different system parameters against the heat sink working fluid inlet temperature in the different heat capacities rate of the heat source are shown. As can be seen, in all graphs with increasing the heat sink working fluid temperature, maximum output power,

Stirling thermal efficiency, dish system efficiency and entropy generation decrease. In Addition, at the given heat sink working fluid inlet temperature all four discussed parameters are increased with increasing in the heat capacities rate of the heat source.

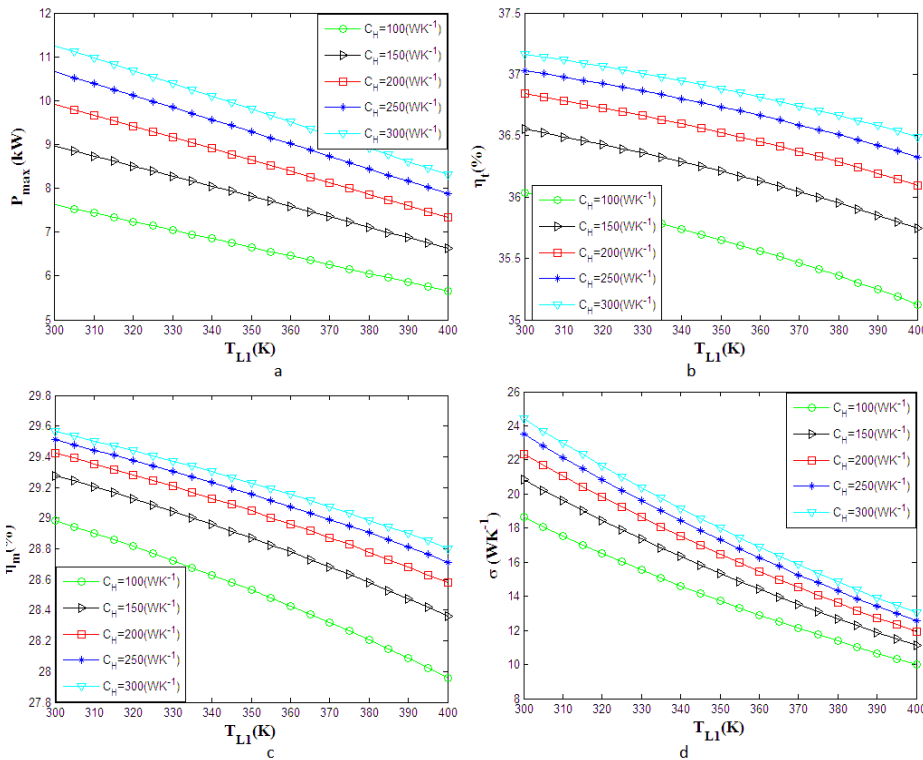


**Figure 8.** Variation of (a) maximum output power, (b) Stirling thermal efficiency, (c) thermal efficiency of the dish system and (d) entropy generation and heat sink working fluid inlet temperature at a different heat capacities rate of heat source

From Figure 9 all parameters in Figure 8 are illustrated for the heat capacities rate of the heat sink. Similarly all parameters express same manner versus the heat sink working fluid inlet temperature. Also at given heat sink

working fluid inlet temperature, all parameters increase with increasing the in the heat capacities rate of the heat sink.

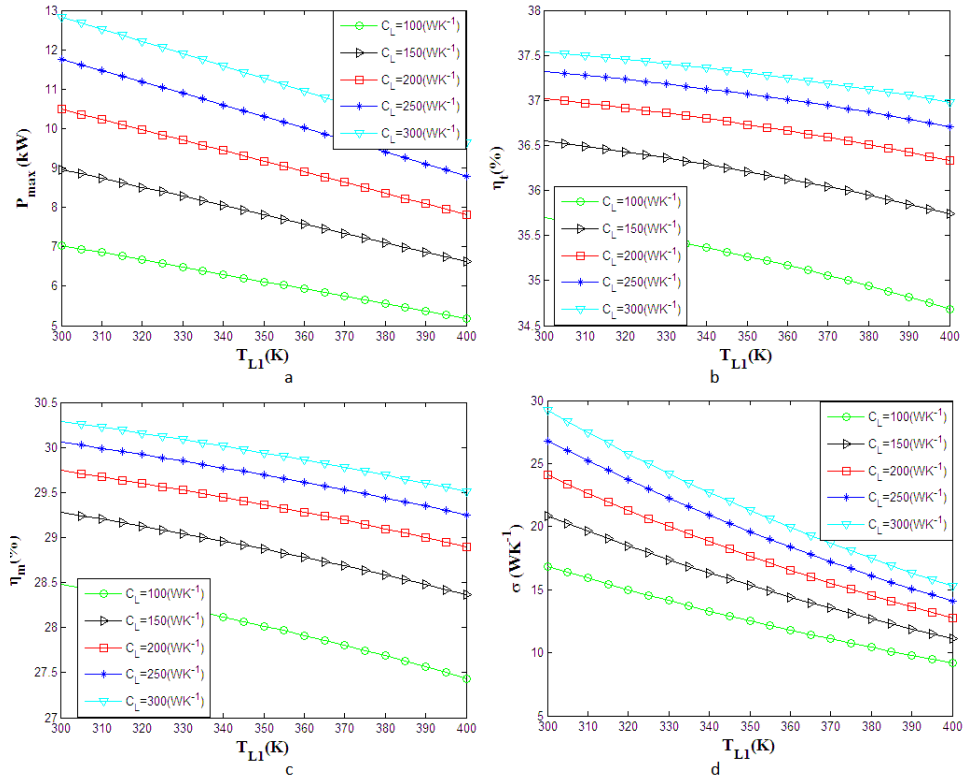


**Figure 9.** Variation of (a) maximum output power, (b) Stirling thermal efficiency, (c) thermal efficiency of the dish system and (d) entropy generation and heat sink working fluid inlet temperature at different heat capacities rate of heat sink

From Figure 10 it can be observed that, the maximum output power, the thermal efficiency, the dish system efficiency and entropy generation decrease with increasing of the heat sink working fluid inlet temperature at

different values of the hot side heat exchanger effectiveness. Moreover, at given heat sink working fluid inlet temperature, all parameters increase by increasing of the hot side heat exchanger effectiveness from 0.4 to 0.8.

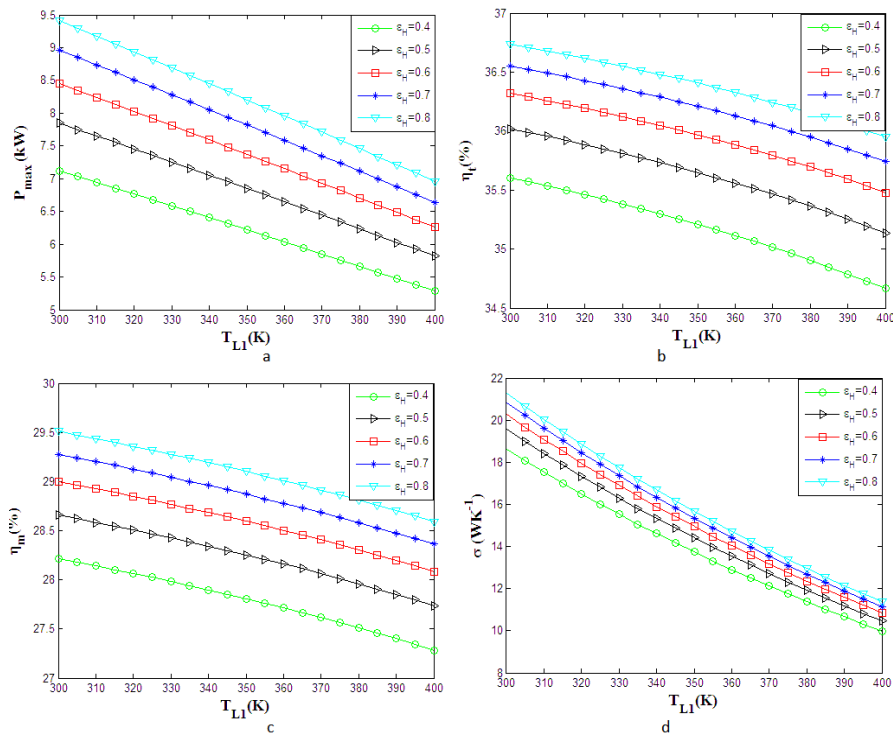


**Figure 10.** Variation of (a) maximum output power, (b) Stirling thermal efficiency, (c) thermal efficiency of the dish system and (d) entropy generation with heat sink working fluid inlet temperature at the different effectiveness of the hot side heat exchanger

In the Figure 11 the similar considered parameters in the Figure 10 are scheming against the heat sink working fluid inlet temperature at the different effectiveness of the

cold side heat exchanger. As it can be pictured overall trends are the same as Figure 10.

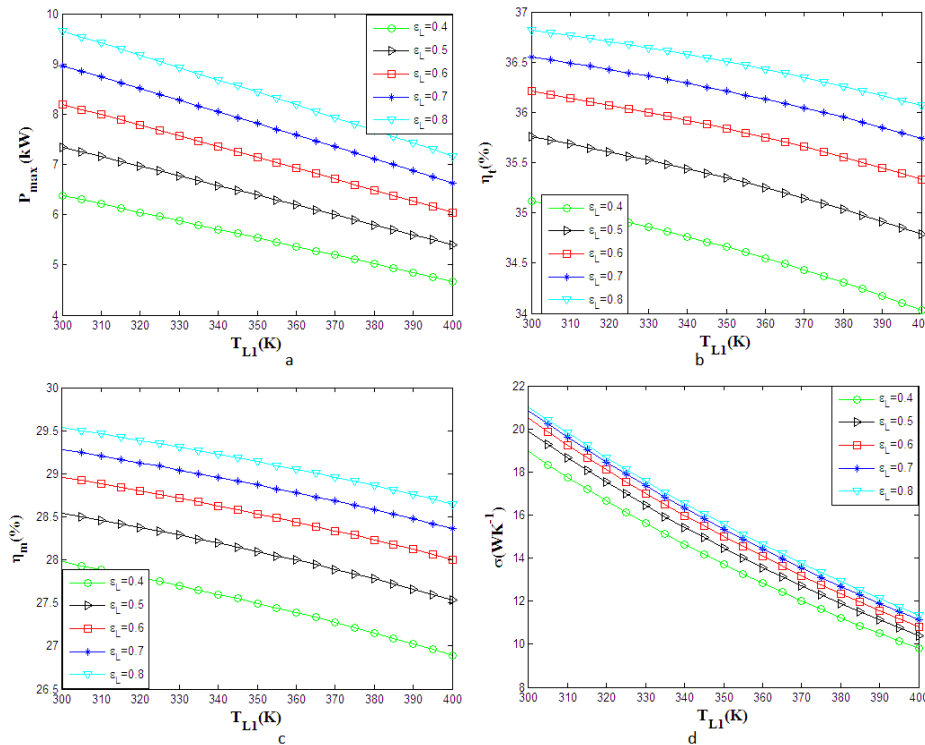


**Figure 11.** Variation of (a) output power, (b) Stirling thermal efficiency, (c) thermal efficiency of the dish system and (d) entropy generation with heat sink working fluid inlet temperature at the different effectiveness of the cold side heat exchanger

## 5. Conclusions

FTT modeling of the solar-dish Stirling engine was performed. In the model non-ideal performance of the regenerator, finite time heat transfer in the heat exchangers, conductive/radiative heat transfers in the absorber (heat source), conductive heat transfer in the heat sink and conductive thermal bridge loss between the heat source and heat sink were taken into account. Finite time thermodynamic analysis has been accepted a straightforward approach for optimization of thermodynamic systems. In the present work sensitivity of different engine's parameters in order to investigate the behavior of the various Stirling system parameters are analyzed. This analysis it also can be applied in determining the function of other related variables such as the volume ratio and the temperature ratio.

The results show parameters such as the heat capacity rate of heat source and heat sink and fluid temperature of the heat source and heat sink play an important role in system design. Also, the presented thermodynamic model is valuable for the design and analysis of the dish-Stirling.

## References

- [1] G Walker. Stirling engines. Oxford: Clarendon Press; 1980 p. 24-5, see also pages 50, 52, 73.
- [2] WB Stine. Stirling engines. In: Kreith F, editor. The CRC handbook of mechanical engineers. Boca Raton: CRC Press; 1998. p. 8-67 see also pages 8-76.
- [3] Schmidt, Theorie der geschlossenen calorischen Maschine von Laubroyund Schwartzkopff in Berlin, Z. Ver. Ing., 1861, 79p.
- [4] G. Walker, Stirling-cycle machines, Clarendon Press, Oxford, 1973, 156 p.
- [5] JR. Senft, An ultra-low temperature differential Stirling engine, Proceeding of the fifth international Stirling engine conference, Paper ISEC 91032, Dubrovnik, May 1991.
- [6] JR. Senft, Mechanical Efficiency of Heat Engines, Cambridge University Press, 2007.
- [7] JR. Senft, Theoretical Limits on the Performance of Stirling Engines, International Journal of Energy Research Vol. (22), 1998, P. 9 91-1000.
- [8] AJ. Organ, The Regenerator and the Stirling Engine, Mechanical Engineering Publications Limited, London, 1997.
- [9] AJ. Organ, Stirling air engine thermodynamic appreciation, J. Mechanical Engineering Science: Part C, 214, 2000, P. 511-536.
- [10] Formosa, F., G. Despesse., Analytical model for Stirling cycle machine designs. Energy Conversion and Management, 51, 2010, P. 1855-1863.
- [11] Thombare, D.G, S.K. Verma., Technological development in the Stirling cycle engines. Renewable and sustainable Energy Reviews, 12, 2008, P. 1-38.
- [12] AR. Tavakolpour, A. Zomorodian, AA. Golneshan. Simulation construction and testing of a two-cylinder solar Stirling engine powered by a flat-plate solar collector without regenerator. Renewable Energy, 33, 2008, P. 77-87.
- [13] M.H. Ahmadi, H. Hosseinzade, Investigation of Solar Collector Design Parameters Effect onto Solar Stirling Engine Efficiency, Applied Mechanical Engineering, 1, 2012, 1-4.
- [14] D.J. Shendage, S.B. Kedare, S.L. Bapat, An analysis of beta type Stirling engine with rhombic drive mechanism, Renewable Energy, 36 (1), 2011, 289-297.
- [15] E. Eid, Performance of a beta-configuration heat engine having a regenerative displacer, Renewable Energy, vol. 34 (11), (2009), 2404-2413.
- [16] E. Podesser, "Electricity Production in Rural Villages with Biomass Stirling Engine", Renewable Energy, 16 (1-4), 1999, 1049- 1052.
- [17] M Costa, M Feidt. the effect of the overall heat transfer coefficient variation on the optimal distribution of the heat transfer

- surface conductance or area in a Stirling engine. *Energy Convers Manage* 39, 1998, 1753-63.
- [18] K. Makhkamov and D. B. Ingham, "Analysis of the working process and mechanical losses in a Stirling engine for a solar power unit," *ASME J. Sol. Energy Eng.* 122 (2000), 208.
- [19] N. Parlak. Thermodynamic analysis of a gamma type Stirling engine in non-ideal adiabatic conditions. *Renewable Energy* 34 (1), (2009), 266-73.
- [20] C Cinar, S Yucesu, T Topgul, M Okur. Beta-type Stirling engine operating at atmospheric pressure. *Appl Energy* 81, (2005), 351-7.
- [21] A. Minassians, SR. Sanders, Stirling engine for Distributed low-Cost Solar-Thermal-Electric Power Generation, *Journal of Solar Energy Engineering: ASME*, 133, 2011, 011015-2.
- [22] A Robson, T Grassie, J Kubie. Modelling of a low temperature differential Stirling engine. *Proceedings of the Institution of Mechanical Engineers, Part C: Journal of Mechanical Engineering Science* 221, 2007, 927-943.
- [23] B Kongtragool, S Wongwises. Thermodynamic analysis of a Stirling engine including dead volumes of hot space, cold space and regenerator. *Renew Energy* 31, (2006), 345-59.
- [24] B Kongtragool, S Wongwises. Investigation on power output of the gamma-configuration low temperature differential Stirling engines. *Renewable Energy* 30, (2005), 465-76.
- [25] B Kongtragool, S Wongwises. Optimum absorber temperature of a once-reflecting full conical concentrator of a low-temperature differential Stirling engine. *Renewable Energy* 31, (2006), 345-59.
- [26] S Abdullah, BF Yousif, K Sopian. Design consideration of low temperature differential double-acting Stirling engine for solar application. *Renew Energy* 30, (2005), 1923-41.
- [27] M Costa, S Petrescu, C Harman. The effect of irreversibilities on solar Stirling engine cycle performance. *Energy Convers Manage* 40, (1999), 1723-31.
- [28] Y Timoumi, I Thili, S Ben Nasrallah. Design and performance optimization of GPU-3 Stirling engines. *Energy* 33 (7), (2008), 1100-14.
- [29] WR Martini. Stirling engine design manual. NASA CR-168088; 1983.
- [30] Percival WH. Historical review of Stirling engine development in the United States from 1960 to 1970. NASA CR-121097; 1974.
- [31] B. Andresen, RS. Berry, A Nitzan and P Salamon, Thermodynamics in finite time. I. The step Carnot cycle, *Phys Rev A*, 15, (1977), pp. 2086-93.
- [32] Chen L, Wu C, Sun F. Finite time thermodynamics optimization or entropy generation minimization of energy systems. *J Non-Equilibrium Thermodyn* 1999; 24: 327.
- [33] S. Petrescu, M. Costea, G. Stanescu., Optimization of a cavity type receiver for a solar Stirling engine taking into account the influence of the pressure losses, finite speed losses, friction losses and convective heat transfer, *ENSEC' 93*, Cracow, Poland, 1993.
- [34] HG Ladas, OM Ibrahim, Finite-time view of the Stirling engine, *Energy*, 19 (8), (1994), pp. 837-43.
- [35] Ahmadi MH, GhareAghaj SS, Nazeri A. Prediction of power in solar Stirling heat engine by using neural network based on hybrid genetic algorithm and particle swarm optimization. *Neural Comput & Applic* 2013; 22: 1141-50.
- [36] Ahmadi MH, Sayyaadi H, Dehghani S, Hosseinzade H. Designing a solar powered Stirling heat engine based on multiple criteria: maximized thermal efficiency and power. *Energy Convers Manage* 2013; 75: 282-91.
- [37] Ahmadi MH, Mohammadi AH, Dehghani S, Barranco-Jiménez Marco A. Multiobjective thermodynamic-based optimization of output power of solar dish- Stirling engine by implementing an evolutionary algorithm. *Energy Convers Manage* 2013; 75: 438-45.
- [38] DA Blank, C Wu. Power optimization of an extraterrestrial solar-radiant Stirling heat engine. *Energy* 20 (6), (1995), 523-30.
- [39] L. Yaqi and et al, Optimization of solar-powered Stirling heat engine with finite-time thermodynamics, *Renewable Energy*, 36 (2011), pp. 421-427.
- [40] I Thili, "Finite time thermodynamic evaluation of endoreversible Stirling heat engine at maximum power conditions", *Renew & Sustain Energy Review*, 16 (4), 2012, 2234-2241.
- [41] SC Kaushik, S Kumar, Finite time thermodynamic evaluation of irreversible Ericsson and Stirling heat engines, *Energy Convers Manage*, 42 (2001), pp. 295-312.
- [42] SC Kaushik, S Kumar, Finite time thermodynamic analysis of endoreversible Stirling heat engine with regenerative losses, *Energy*, 25 (2000), pp. 989-1003.

### Nomenclature

$A$	Area, m <sup>2</sup>
$C$	Heat capacitance rate, WK-1
$C_v$	Specific heat capacity, Jmol-1K-1
$K_0$	Heat leak coefficient, WK-1
$n$	Number of mole
$N$	Number of heat transfer units
$P$	Power output, W
$Q$	Heat, J
$R$	The gas constant, Jmol-1K-1
$S$	Entropy, JK-1
$T$	Temperature, K
$t$	Time, s
$U$	Overall heat transfer coefficient, WK-1m-2
$V$	Volume of the working fluid, m <sup>3</sup>
$W$	Output work, j
Subscripts	
$L$	Cold side/Heat sink
$H$	Heat source
$h$	Hot side
1	Inlet
2	Outlet
1, 2, 3, 4	State points
$R$	Regenerator
Greek	
$\lambda$	Ratio of volume during the regenerative processes
$\varepsilon$	Effectiveness and emissivity factor
$\eta$	Thermal efficiency
$\sigma$	entropy production